Desalination and Water Treatment
www.deswater.com

doi: 10.5004/dwt.2017.21225

90 (2017) 180–188
September

Comparison of catalytic effect of Fe-MOF and Fe-ZIF for Fenton degradation of Eriochrome black T

Elham Hadinejad[a], Saeedeh Hashemian[a,*] S. Ali Yasini[b]

[a]*Department of Chemistry, Islamic Azad University, Yazd Branch, Yazd, Iran, Tel. +98 31872752; Fax: +983537266065; emails: sa_hashemian@iauyazd.ac.ir (S. Hashemian), elhadinejad@gmail.com (E. Hadinejad)*

[b]*Department of Food Science and Technology, Islamic Azad University, Yazd Branch, Yazd, Iran, email: sa.yasini@yahoo.com*

Received 16 January 2017; Accepted 15 July 2017

ABSTRACT

Fe-MOF and Fe-ZIF as heterogenic catalysts were prepared and characterized by FTIR, X-ray diffraction and scanning electron microscopy methods. The decolorization of Eriochrome black T (EBT) by Fenton oxidation was investigated. The effects of different parameters such as contact time, amount of catalyst, pH of solution, the initial concentrations of Fe^{2+}, H_2O_2 and EBT dye on the oxidation were investigated and optimized conditions were determined. The 95% degradation of EBT was obtained after 15 min of reaction at pH 3 for EBT 60 mg L^{-1} and 0.04 g catalyst. Results showed that efficiency of EBT removal is as followed: Fe^{+2}/H_2O_2 < Fe^{+2}/H_2O_2/Fe-MOF < Fe^{+2}/H_2O_2/Fe-ZIF. Results of TOC removal showed the partial and insignificant mineralization of EBT (85%). The results of experiments showed that degradation of EBT dye described with a pseudo-second-order kinetic model. The catalysts could be easily recovered and showed high potential for applications in wastewater treatment without secondary pollution. In conclusion, heterogen catalysts of Fe-MOF and Fe-ZIF for Fenton oxidation method as promising technique can provide appropriate conditions for the treatment of dye for the reuse of effluents.

Keywords: Catalyst; Eriochrome black T; Fenton; MOF; Oxidation; ZIF

1. Introduction

Many organic compounds, particularly dyes and aromatic hydrocarbons, are widely used in the chemical industry. Most of dyes are toxic and they often represent serious environmental hazards. Removal of dyes from industrial effluent is environmentally important and they must be removed before discharge into receiving streams. Numerous industries like textile, paper, pulp, dyeing and printing industries are throwing their effluents into water bodies and causing water pollution. Effluents of textile industries contain dyes that make the water colored and toxic and thus making it unfit for any use [1,2]. Azo dyes are characterized by the nitrogen double bond (–N=N–) which together with other chromophores is responsible for the color. Azo dyes are typically used in textile processing and paper manufacturing industries. A massive amount of azo dyes from these sources is discharged into natural waterways [3]. From an environmental point of view, the removal of synthetic dyes is of great concern. Biological treatment is one of treatment methods for wastewater containing organic compounds and dyes. Many synthetic dyes do not easily decompose in biological treatments due to their toxic effects on microorganisms.

The removal of dyes from aqueous solutions by physical and chemical methods such as coagulation, oxidation, photocatalysis, adsorption, nanofiltration, micellar-enhanced ultrafiltration, and so on, has been widely studied [4–11]. Physical and chemical processes (e.g., adsorption, coagulation/flocculation and membrane separation) only transfer the pollutants from one phase to the other [12,13]. These methods are either costly, inefficient or result in the production of secondary toxic waste products.

* Corresponding author.

The advanced oxidation processes (AOPs), based on the generation of highly reactive and non-selective hydroxyl radicals ($HO^{\bullet}$), are among the most promising techniques for the removal of recalcitrant organics. AOPs allow for the effective oxidation of many organics, in some cases, up to H_2O and CO_2 (i.e., with complete mineralization).

Oxidation by Fenton (Fe^{2+}/H_2O_2) reactions is proven to be an economically feasible process for destruction of a variety of hazardous pollutants in wastewater.

Fenton process, an important AOP technology, has been attracting growing interest. It is well known that ^{-}OH radicals can be produced by Fenton's reaction of H_2O_2 with Fe^{2+} and Fe^{3+} salts as presented in the following equations:

$$Fe^{2+} + H_2O_2 + H^+ \rightarrow Fe^{3+} + H_2O + {}^{\bullet}OH \quad (1)$$

$$Fe^{3+} + H_2O_2 \rightarrow Fe^{2+} + HO_2^{\bullet} + H^+ \quad (2)$$

$$Fe^{3+} + H\,O_2^{\bullet} \rightarrow Fe^{2+} + H^+ + O_2 \quad (3)$$

Recently, homogeneous Fenton's process is one of the most interesting AOPs due to the low investment cost and the easiness of implementation. Degradation of different dyes in aqueous solutions by the Fenton process was reported [14,15].

Eriochrome black T (EBT) is an azo dye. The oxidative removal of EBT from aqueous solutions was also studied [16–18].

The homogeneous Fenton's process entails some disadvantages such as the need of high concentrations of iron in solution and the following effluent treatment for catalyst recovery before discharge. Furthermore, processing of the generated sludge (rich in iron hydroxides) requires large amounts of chemicals and man power, making the process laborious and economically unattractive. To minimize these disadvantages, various studies have investigated the catalytic oxidation as an alternative to the incineration process to destroy dyes and organic compounds.

It is clear that the catalytic oxidation perhaps efficient on the complete oxidation of organic compounds and dyes and preventing the formation of harmful by-products. In heterogenic Fenton reactions, the iron species are attached to a solid porous matrix of catalyst and preventing their loss to the effluent [19,20]. The process is generally complex due to simultaneous adsorption and catalysis phenomena. Eqs. (4) and (5) briefly describe the main reactions involved:

$$S + Fe^{2+} + H_2O_2 \rightarrow S - Fe^{3+} + HO + HO^{-} \quad (4)$$

$$S - Fe^{3+} + H_2O_2 \rightarrow S - Fe^{2+} + HO_2^{\bullet} + H^+ \quad (5)$$

where S represents the surface of the solid matrix. Literature shows several studies where the heterogeneous Fenton's process has been applied for dye removal and textile effluent treatment in either batch [21–23].

Metal–organic frameworks (MOFs) are a class of hybrid materials that are constructed by metal nodes and organic linkers forming highly porous structures. MOFs were used as heterogeneous catalysts for oxidation reactions [24–26], as membrane [27] and energy storage [28]. Iron-terephthalic acid MOF was used as shape and size control catalyst [29].

Zeolitic imidazolate frameworks (ZIFs) are microporous materials and belong to the new class of MOFs. MOFs actually can be alternative catalysts to activate the oxidants for generation of free radicals and only a few studies have evaluated MOFs as catalysts in the wet chemical oxidation reactions. Some of ZIFs were used for the environmental applications to degrade organic pollutants. Recently, ZIFs were used as catalyst for organic reactions [30,31] and degradation of dye [32].

The aim of this study is to synthesize the Fe-MOF and Fe-ZIF as heterogen catalysts for Fenton degradation of EBT. The influences of various parameters on the catalytic degradation of EBT dye by the Fenton process in aqueous solution were investigated to determine the optimal operating conditions for a better performance of the degradation.

2. Experimental

2.1. Materials and methods

All chemicals used were of analytical grade purity and were used as received without any purification. All the chemicals were purchased from Merck Chemical Co. (Germany). Distillated water was used in all the experiments. 1,4-benzenedicarboxylic acid (H2PBC), and 2-methyl imidazole were used as linker for preparation of Fe-MOF and Fe-ZIF, respectively.

Eriochrome black-T (1-Naphthalenesulfonic acid, 3-hydroxy-4-[(1-hydroxy-2-naphthyl)azo]-7-nitro-, sodium salt), CAS number 1787-61-7 with chemical formula of $C_{20}H_{12}N_3O_7SNa$ (EBT) as a sample of pollutant was used. It has molecular weight of 461.380 g mol^{-1} (Fig. 1). The standard solution of EBT 500 mg L^{-1} was prepared and diluted subsequently whenever necessary.

All the experiments were conducted at room temperature. The oxidation of EBT was considered by Fenton reagent, which was composed of a mixture of $FeSO_4{\cdot}7H_2O$ and H_2O_2 (30%). The experiments were studied in presence and absence of Fe-ZIF and Fe-MOF as heterogenic catalysts.

The necessary quantities of Fe^{2+} and H_2O_2 were added simultaneously in the dye solution. All experiments were conducted in a 500 mL thermostated batch glass reactor equipped with the magnetic stirrer. The residual concentration of EBT in the solution at different conditions was determined. The residual concentration of the dye was deducted from the calibration curves, which were produced at wavelength corresponding to the maximum of absorbance (530 nm) on an UV–visible spectrophotometer. Relative standard deviation (%) was determined between 1.92% and 2.65% for each points at all the experiments.

The discoloration efficiency of the dye (Y) with respect to its initial concentration is calculated as:

$$\%\ Y = ([EBT]_0 - [EBT]/[EBT]_0) \times 100 \quad (6)$$

where $[EBT]_0$ and [EBT] are the initial and appropriate concentrations of dye, respectively.

2.2. Synthesis of Fe-MOF and Fe-ZIF

Fe-MOF (Fe-1,4-benzenedicarboxylic acid) and Fe-ZIF (Fe-2-methyl imidazole) were prepared and characterized.

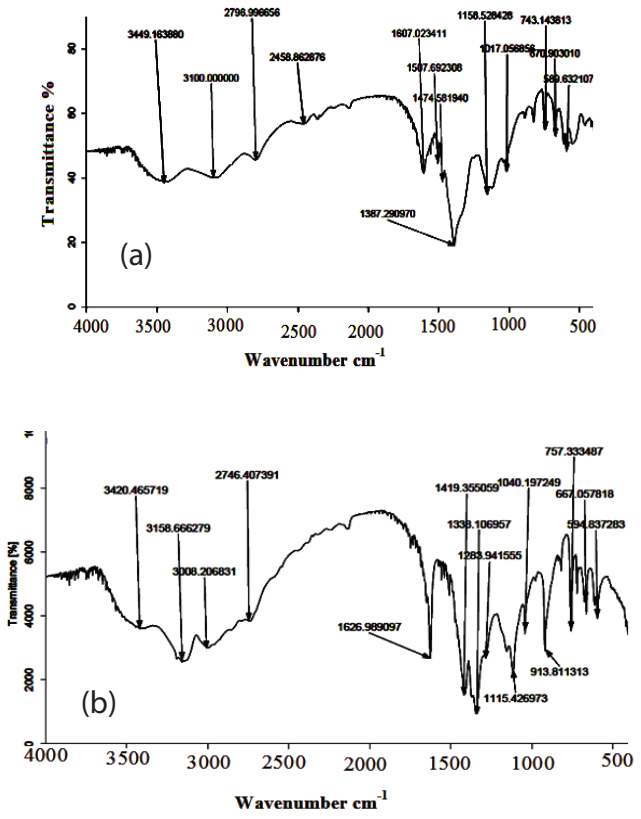

Fig. 1. FTIR of a-Fe-MOF and b-Fe-ZIF.

In total, 1 mmol of iron(II) nitrate hexahydrate ($Fe(NO_3)_2.7H_2O$, 0.405 g) was dissolved at 5 mL of dimethyl foramide (DMF) (A) and 1 mmol of 1,4 benzenedicarboxylic acid (0.166 g) separately was dissolved in DMF (B). Then, A solution was added to B solution and pH was adjusted by trimethyl amine from 3 to 5. The mixed solution was kept at 70°C for 15 min and then cooled at room temperature. The precipitate was washed by ethanol and dried at 50°C for 60 min. The prepared compound called Fe-MOF.

Then, 4 mmol of iron(II) nitrate hexahydrate (1.62 g) and 16.4 mmol of 2-methylimidazole (2.985 g) were dissolved separately in about 9 mL DMF. The solutions were mixed and then stirred for ~6 h, and vigorously centrifuged at 3,000 rpm. The prepared compound washed thoroughly with methanol. This washing procedure was repeated three times. The red-brown crystals were separated from the mother liquid, washed thrice with 3 mL DMF, and allowed to dry in air. The resultant crystals were dried overnight at 80°C and called Fe-ZIF.

2.3. Characterization of catalyst

UV–Vis spectrophotometer 160-A Shimadzu was used for determination of concentration of EBT. The cells used were in quartz 1 cm thick. IR measurements were performed by FTIR tensor-27 of Burker Co., using the KBr pellet between the ranges of 500–4,000 cm^{-1}. The powder X-ray diffraction studies were made on a Philips PW1840 diffractometer using Ni-filtered Cu k_α radiation. The average particles size and morphology of samples were observed by scanning electron microscope (SEM) using a Hitachi S-3500.

3. Results and discussion

3.1. Characterization of catalyst

Fig. 1 shows the FTIR spectra of the Fe-MOF (a) and Fe-ZIF (b). The IR analyses indicated strong and broad peak located about 3,410 cm^{-1} is assigned to the O–H vibration, indicating the presence of water. The FTIR spectra illustrated peak at close to 580 cm^{-1} which corresponded to its Fe–O band [33]. In the FTIR spectra of Fe-MOF, the absorption at 1,607 is assigned to C=O band, the bands of 2,924 and 3,085 cm^{-1} are derived from the C–H stretching of aromatic rings and the bands of 1,474, 1,507 and 1,387 cm^{-1} are owing to O–C–O band stretching. The bands at 670,743 cm^{-1} can be allocated to the out-of-plane bending vibrations of benzene rings [33]. These results suggest that the structure of Fe-MOF contains the basic H2PBC skeleton and the carboxyl groups of H2PBC are deprotonated. The C–H stretch vibration occurs about 3,100–3,130 cm^{-1}. The C=C stretch band of aromatic ring is around 1,600–1,500 cm^{-1} (Fig. 1(a)). The absence of the absorption bands in the region of 1,680–1,800 cm^{-1} is in accord with complete H2PBC ligand deprotonation [34].

FTIR spectra of the Fe-ZIF (Fig. 1(b)) showed a significant difference from that of the 2-methylimidazole linker. In the FTIR spectra of 2-methylimidazole, a strong and broad band from 3,400 to 2,200 cm^{-1} with the maximum at 2,650 cm^{-1} was assigned to the N–H···N hydrogen bond. The resonance between the N–H···N out-of-plane bending and the N–H stretching vibrations was found at 1,846 cm^{-1}. These absorption bands were not seen in the spectra of the Fe-ZIF, confirming that 2-methylimidazole linker was fully deprotonated during the formation of the ZIF structure.

XRD pattern of the Fe-MOF is shown in Fig. 2(a). The main diffraction peaks of the Fe-MOF sample are observed at 2θ values of approximately 7.5°, 10.2°, 12.6°, 13°, 14.4°, 18° and 19.7°. The XRD pattern of the Fe-MOF is consistent with that of the Fe-MOF prepared by Yin et al. [35].

A very sharp peak below 10° in Fig. 2(b) (2θ of 7.2) was observed in the XRD pattern of the Fe-ZIF, indicating that a highly crystalline material was achieved [36].

The overall XRD patterns of the Fe-ZIF in this work were in good agreement with the patterns from single crystal data. It was apparent that the ZIF had better crystallinity as compared with silica-based materials such as Al-MCF and SBA-15 where broader peaks were observed on their diffractograms [37–39].

The average crystalline size of the samples was calculated according to Debye–Scherrer formula:

$$D = 0.9\,\lambda/\beta\cos\theta \quad (7)$$

where D is the average crystallite size (Å), λ is the wavelength of the X-ray radiation (Cu K_α = 1.5418 Å), β is the full width at half maximum (FWHM) intensity of the peak and θ is the diffraction angle. The mean particle size of Fe-MOF and Fe-ZIF were calculated by Scherrer equation 30–40 nm and 25–30 nm, respectively.

Scanning electron microscopy was used to study the surface morphology and the pore size of the samples. The SEM

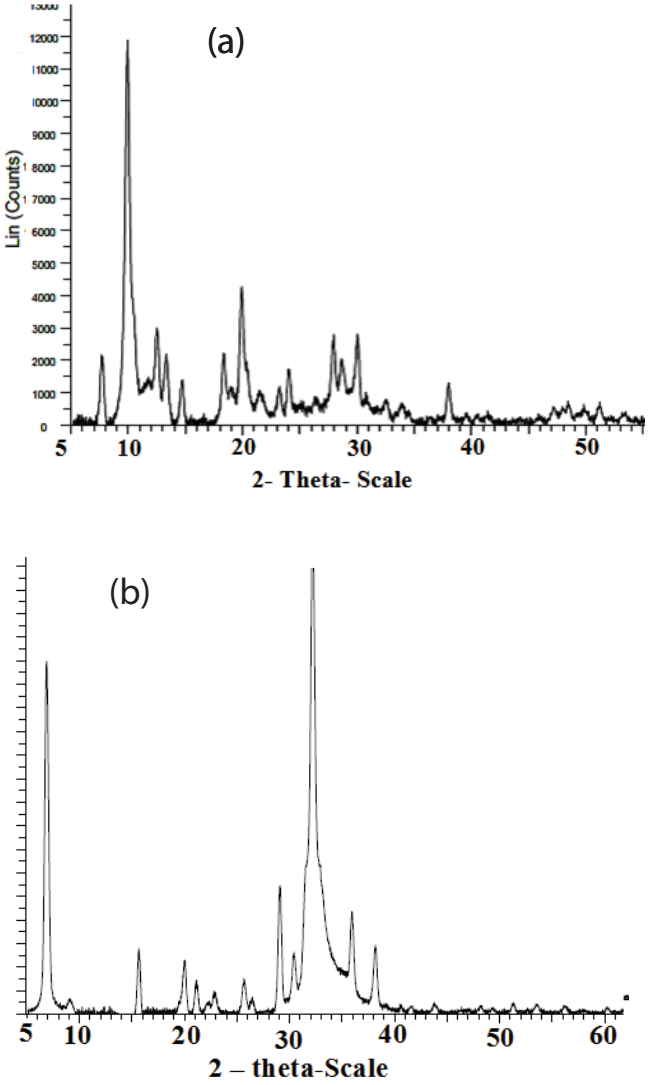

Fig. 2. (a) XRD patterns of Fe-MOF; (b) XRD patterns of Fe-ZIF.

analysis revealed that the Fe-MOF and Fe-ZIF possessed a porous structure.

As shown in Fig. 3, the size of nanoparticles of Fe-MOF and Fe-ZIF were determined about 35 and 25 nm, respectively. Moreover, as it is shown, Fe-MOF nanoparticles had spherical shapes, but Fe-ZIF nanoparticles had hexagonal forms.

Based on the EDX results, the elementary analysis of Fe-MOF and Fe-ZIF were determined. The elements, percentage mass of elements existing in Fe-MOF and Fe-ZIF are summarized in Table 1.

3.2. Degradation of EBT

In a typical experiment, a specific amount of catalyst was added into 20 mL of EBT 60 mg L^{-1}. All the experiments were carried out in 150 mL conical flask and the flask was covered with foil to exclude the impact of light.

The adjacent temperatures were controlled at 25°C ± 1°C. The EBT stock solution with a concentration of 500 mg L^{-1} was freshly prepared by dissolving an exact amount of EBT into purified water.

3.2.1. Effect of catalyst

Fenton reactions were performed for EBT degradation. Fenton reaction based on ferrous ions and hydrogen peroxide is showed to be an effective method to degrade organic pollutants. No acid or base was used to adjust the pH value of the reaction solution and all reactions were carried out in the dark to avoid the influence of light. To increase rate

Table 1
EDX (atomic %) data for Fe-MOF and Fe-ZIF

Sample	C	O	N	Fe
Fe-MOF	40.46	33.23	24	2.23
Fe-ZIF	29.98	28.66	37.69	3.67

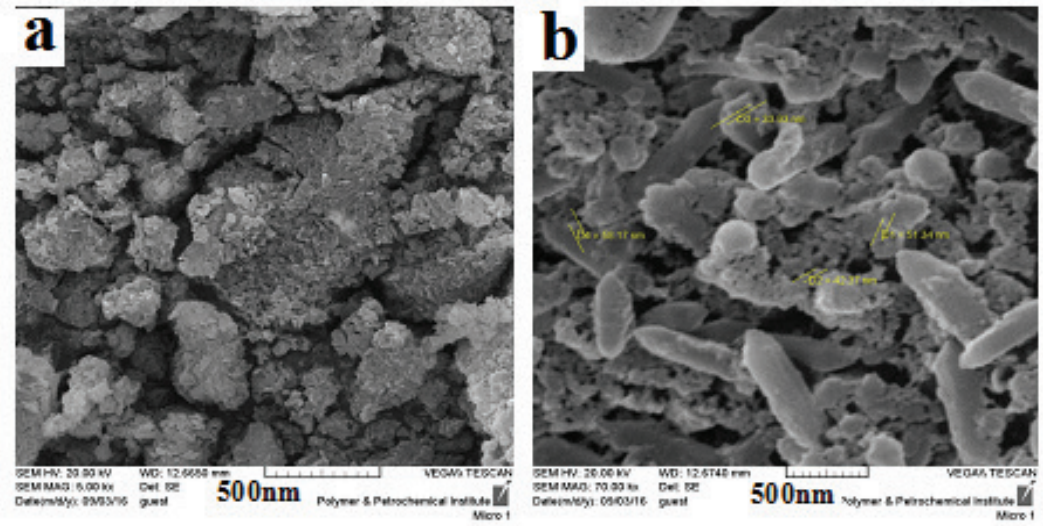

Fig. 3. SEM image of (a) Fe-MOF and (b) Fe-ZIF.

and efficiency of oxidation of EBT and overcome the difficulty of separation of iron homogeneous catalysts, Fe-MOF and Fe-ZIF were used as heterogeneous Fenton catalysts. The degradation of EBT by Fe/H_2O_2 was nearly low and maximum removal of EBT dye was 54%. In Fenton's oxidation process, only hydroxyl radicals generated from the catalytic decomposition of H_2O_2 are able to oxidize EBT (Fig. 4(a)).

In heterogeneous catalyst of Fenton reaction, 75% after 20 min and 90% after 15 min of EBT was degraded on Fe-MOF and Fe-ZIF, respectively. The results showed that the Fe-ZIF had higher catalytic activity than Fe-MOF for degradation of EBT. It may be due to porous nature and smaller particle size of Fe-ZIF. Process could be divided into two steps, a quick step and a slow one. In the first step, the rate of oxidation was very fast, and about 90% of the oxidation was achieved within 20 min. In the subsequent step, the oxidation was slow and reached equilibrium at longer time (40 min). As a result, higher oxidation efficiency was realized in a shorter time.

In heterogeneous Fenton process, iron salts were adsorbed onto the surface of supported catalysts, and in a suitable aqueous medium, the reduction–oxidation reactions between Fe^{+2}/Fe^{+3} happen in the presence of hydrogen peroxide which promote the formation of reactive components such as ($^{\bullet}OH$) and hydroperoxyl ($^{\bullet}OOH$) radicals. The radicals generated by the decomposition of hydrogen peroxide can oxidize organic compounds adsorbed over the catalyst or degrade soluble organic compounds in the area of active iron ions present at both the catalyst surface and in the bulk liquid phase. Thus, the Fe(III)/Fe(II) complex formed on the surface of support can react with H_2O_2 thus allowing iron ions to participate in the Fenton catalytic cycle. Therefore, the iron species are attached to a solid porous matrix of catalyst (e.g., Fe-MOF and Fe-ZIF) avoiding their loss to the waste. The process is generally complex. Both oxidations, Fenton and adsorption processes, occurred simultaneously in the catalysis system (Fe^{+2}/H_2O_2/Fe-MOF and Fe^{+2}/H_2O_2/Fe-ZIF).

Figs. 4(b) and (c) show the Fenton degradation of EBT using Fe-MOF and Fe-ZIF catalysts. The consequence of degradation of EBT was as followed:

$Fe^{+2}/H_2O_2 < Fe^{+2}/H_2O_2$/Fe-MOF $< Fe^{+2}/H_2O_2$/Fe-ZIF.

3.2.2. Effect of catalyst dosage

The effect of amount of catalyst on the percentage of oxidation and degradation of EBT dye was investigated. The effect of amount of catalyst on the percentage of dye degradation was investigated in the range 0.001–0.015 g. The result is presented in Fig. 5. The result indicated that the degradation of EBT was significantly influenced by the dosage of catalyst and the optimum amount was observed at 0.004 g of catalyst with high decolorization efficiency. An increase in the amount of catalyst dosage will provide more iron sites on the catalyst surface for accelerating the decomposition of H_2O_2 which in turn increase the number of hydroxyl radical significantly.

Results showed with an increase in the amount of catalyst to a certain level (0.004 g), the rate of degradation increases, which may be regarded as a saturation point. This may be also explained by the fact that with an increase in the amount of catalyst, the surface area of catalyst will increase. However, after a certain limiting amount of catalyst, less number of hydroxyl radicals is formed and reaction rate is slow. This is in agreement with the results observed by Zhang et al. [40].

3.2.3. Effect of pH

The effect of initial pH solutions on the degradation of EBT was studied in the pH range of 2.0–6.0 with initial concentration of 60 mg L^{-1} of EBT, Fe^{+2} = 16 mg L^{-1}, H_2O_2 = 4 mg L^{-1}. The results indicated that the decolorization of EBT was significantly influenced by the pH of the solution. At pH 3, the maximum 95% of decolorization efficiency within 20 min reaction time was attained. The EBT removal efficiency was found to get reduced at higher pH values. This may be because at higher pH (above 3), ferrous ions get easily converted to ferric ions, which have a tendency to produce ferric-hydroxo complexes with H_2O_2. The low degradation at pH 2 and 2.5 may be due to the hydroxyl radical scavenging by H^+ ions and also there may be inhibition for the radical forming activity of iron [41]. Thus, subsequent experiments of Fenton oxidation were fixed for pH = 3.

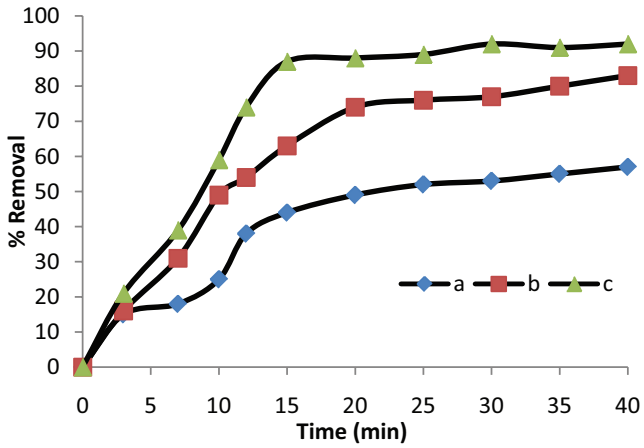

Fig. 4. a-Fe^{+2}/H_2O_2, b-Fe^{+2}/H_2O_2/Fe-MOF, c-Fe^{+2}/H_2O_2/Fe-ZIF (EBT 60 mg L^{-1}, Fe^{+2} = 16 mg L^{-1}, H_2O_2 = 4 mg L^{-1}, 0.001 g catalyst).

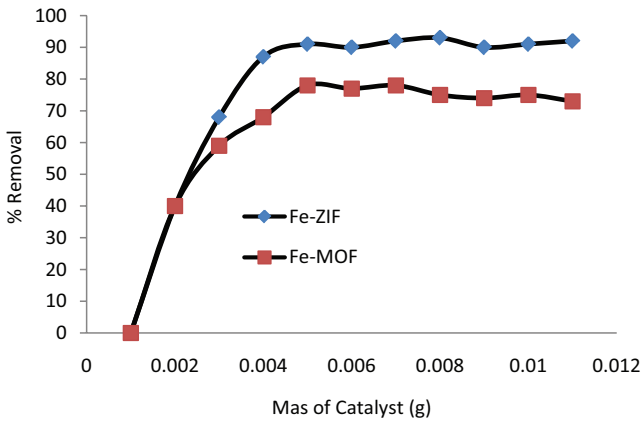

Fig. 5. Effect of catalyst mass for oxidation of EBT (EBT 60 mg L^{-1}, Fe^{+2} = 16 mg L^{-1}, H_2O_2 = 4 mg L^{-1}).

3.2.4. Effect of amount of H_2O_2

H_2O_2 plays the role of an oxidizing agent in the Fenton process. The selection of an optimal H_2O_2 concentration for the decolorization of EBT is important from practical point of view due to the cost of H_2O_2. The effect of H_2O_2 amount on the degradation of EBT was examined by varying initial concentration of H_2O_2 from 0.5 to 15 mg L^{-1}. The result is shown in Fig. 6. The addition of higher content of H_2O_2 leads to accelerating the speed of decolorization of the solution. It can be seen from Fig. 6, the effect of increasing initial concentration from 0.5 to 3 mg L^{-1} was first positive for the degradation of EBT for both catalyst. This is due to the oxidation power of Fenton which was improved with increasing •OH radical amount obtained from the decomposition of increasing H_2O_2. However, with continuous increasing of H_2O_2 concentration more than 4 mg L^{-1}, the decolorization rate of EBT was reduced. This may be explained by the fact that the very reactive •OH radical could be consumed by H_2O_2 and results in the generation of less reactive •OOH [23].

3.2.5. Effect of Fe^{2+} dosage

The Fe^{2+} has a great effect on the efficiency of the Fenton reaction. Therefore, further experiments concern the effect of Fe^{+2} amount on discoloration efficiency. To study the iron concentration, varying initial concentration of Fe^{2+} from 4 to 40 mg L^{-1} was examined. Fig. 7 shows the effect of Fe^{2+} concentration on the degradation of EBT by Fe-MOF and Fe-ZIF. The amount of degradation of EBT increased with increasing Fe^{2+}concentration. An obvious increase of the decolorization efficiency was observed by raising initial Fe^{2+} concentration from 4 to 16 mg L^{-1}. However, further increase in the concentration of Fe^{2+} from 20 to 40 mg L^{-1} did not brought about further improvement in the dye removal. This fact was probably due to the consumption of the percentage of very reactive •OH radical by an excess of ferrous ions, which is necessary to form peroxide radicals (HO_2•). The higher concentration of Fe^{2+} could lead to the self-scavenging of •OH radicals (Eq. (8)):

$$Fe^{2+} + {}^{\bullet}OH \rightarrow Fe^{3+} + {}^{-}OH \quad (8)$$

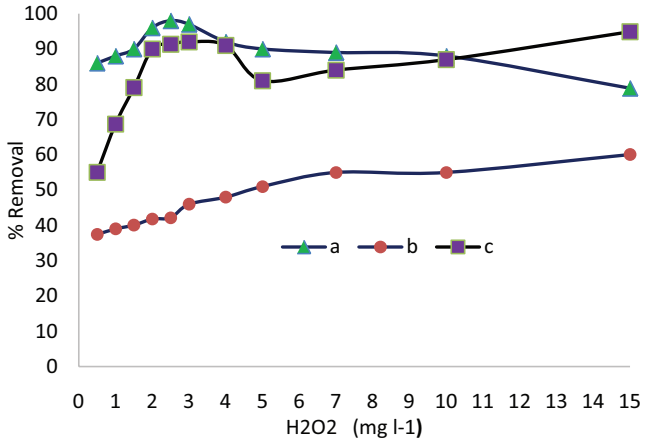

Fig. 6. Effect of amount of H_2O_2 for oxidation of EBT (EBT 60 mg L^{-1}, Fe^{+2} = 16 mg L^{-1}, 0.004 g catalyst).

3.2.6. Effect of concentration of dye

Concentration of dye plays a very important role in reactions according to the collision theory of chemical reactions. The effect of different initial concentration of EBT dye by oxidation process by Fenton reaction was investigated at range of 30–100 mg L^{-1} (Fig. 8). The results showed percentage removal of EBT increased from 30 to 60 mg L^{-1} and then, decreases with increasing initial dye concentration from 60 to 100 mg L^{-1}. By increasing the concentration of reactants, the frequency of collisions between the reactant molecules is increased and the frequency of effective collisions that causes a reaction to occur will also be high. The hydroxyl radicals have very short lifetime and they can only react where they are formed. Therefore, as increasing the amount of dye molecules per volume unit logically increases the probability of collision between dye and oxidizing species, leading to an increase in the decolorization efficiency. At higher concentration of EBT, hydroxyl radicals are not enough for increasing of decolorization of EBT and in addition, catalyst/sorbent has a limited number of active sites, which become saturated after certain concentration [19].

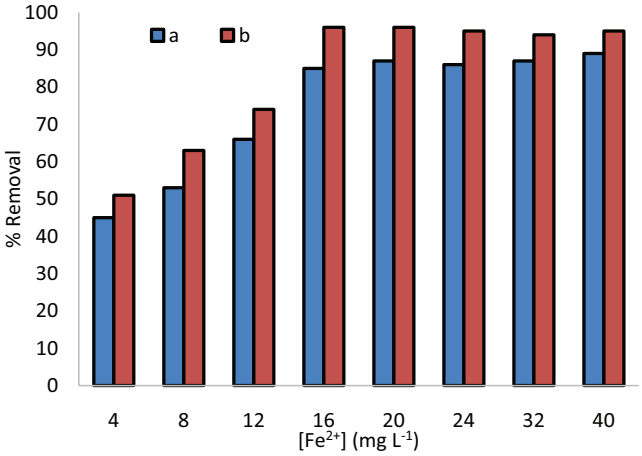

Fig. 7. Effect of Fe^{2+}concentration for oxidation of EBT by a-Fe-MOF and b-Fe-ZIF (EBT 60 mg L^{-1}, H_2O_2 = 4 mg L^{-1}, 0.004 g catalyst).

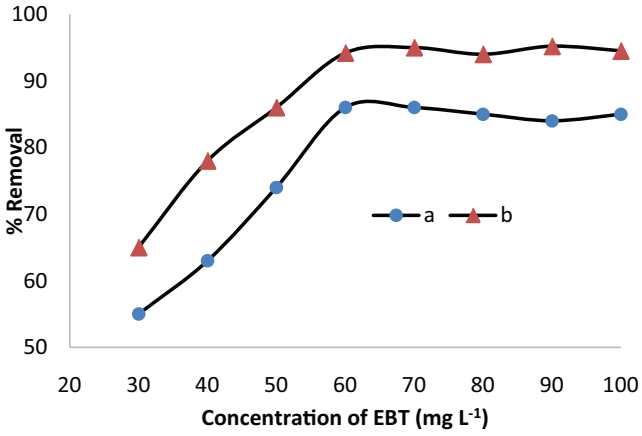

Fig. 8. Effect of concentration of EBT by oxidation for a-Fe-MOF and b-Fe-ZIF.

3.3. Mineralization study

Amount of mineralization of the dye by Fenton process can be evaluated by measuring total organic carbon (TOC). To determine the modification in the TOC of reaction, initial TOC (pure dye solution) and the TOC of a sample at different intervals during the reaction were measured. TOC reduction was determined as follows:

$$TOC_{removal} = (1 - TOC_t)/TOC_0 \times 100 \quad (9)$$

where TOC_t and TOC_0 (mg L^{-1}) are values at time (t) and at time (0), respectively. The depletion in TOC for EBT was investigated. It is shown in Fig. 9 and obviously showed that the reaction does not go to completion. On average, 70% TOC reduction is achieved for EBT dye in 20 min. In fact, after 20 min of reaction, about 75% and 89% (for Fe-MOF and Fe-ZIF, respectively) of the initial organic carbon had been transformed into CO_2, which implied the existence of other organic compounds in the solution and the partial mineralization of dye [42,43].

3.4. Kinetic assessment

The different models were proposed to investigate the kinetic behavior. The kinetic degradation of EBT was investigated by pseudo-first-order and pseudo-second-order models. The rate law of first-order reaction can be written as follows:

$$\ln[C_{EBT}]/\ln[C_{(EBT)0}] = -k_{app}\, t \quad (10)$$

$$\ln[C_{EBT}] = \ln[C_{(EBT)0}] - k_{app}\, t \quad (11)$$

$[C_{EBT}]$ and $[C_{(EBT)0}]$ are initial concentration of EBT and concentration of EBT at the any time. A plot of $\ln[C_{EBT}]$ vs. time generated a straight line with a negative slope. The slope of this line corresponds to the apparent rate constant value for the degradation of EBT (Fig. 10).

The equation of second-order reaction is as follows:

$$1/[C_{(EBT)}]/[C_{(EBT)0}] = k\, t \quad (12)$$

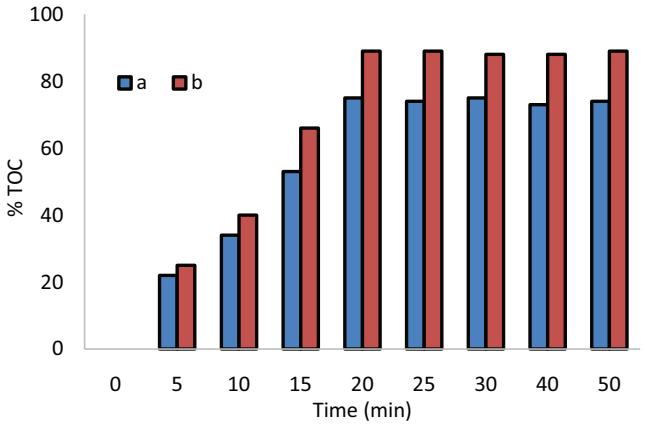

Fig. 9. TOC removal for EBT dye by Fenton oxidation process (a-Fe-MOF, b-Fe-ZIF).

The plot of $1/[C_{EBT}]$ against k shows the rate constant of second-order Fenton reaction (Fig. 11). The results of kinetic parameters are shown in Table 2. The results from R^2 of Figs. 10 and 11 show the kinetic of Fenton reaction for degradation of EBT was followed by second-order reaction [35]. The results showed the Fenton degradation of EBT was slower than catalytic Fenton process. In addition, Fe^{+2}/H_2O_2/Fe-ZIF had higher rate constant than Fe^{+2}/H_2O_2/Fe-MOF.

3.5. Reusability and stability of catalysts

The reuse tests were performed in order to evaluate the catalytic activity of Fe-MOF and Fe-ZIF during successive experiments and thus to observe the possibility of catalyst reuse. The runs were carried out using 100 mL of 60 mg L^{-1} EBT aqueous solution with addition of 4 mg L^{-1} H_2O_2 at a pH of solution. After each run, the catalyst was removed by filtration 1 h. Then, the catalyst was reused with a fresh EBT solution. The results are summarized in Fig. 12. The results show that the catalytic activity decreased slowly during

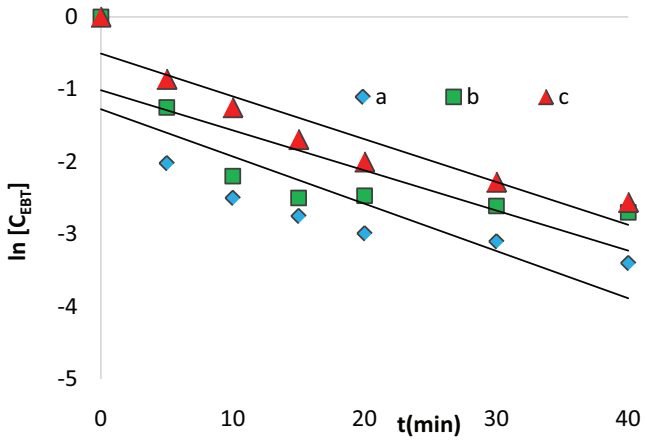

Fig. 10. Pseudo-first-order reaction kinetics for the color removal of EBT a-Fe^{+2}/H_2O_2, b-Fe^{+2}/H_2O_2/Fe-MOF, c-Fe^{+2}/H_2O_2/Fe-ZIF (EBT 60 mg L^{-1}, Fe^{+2} = 16 mg L^{-1}, 0.004 g catalyst).

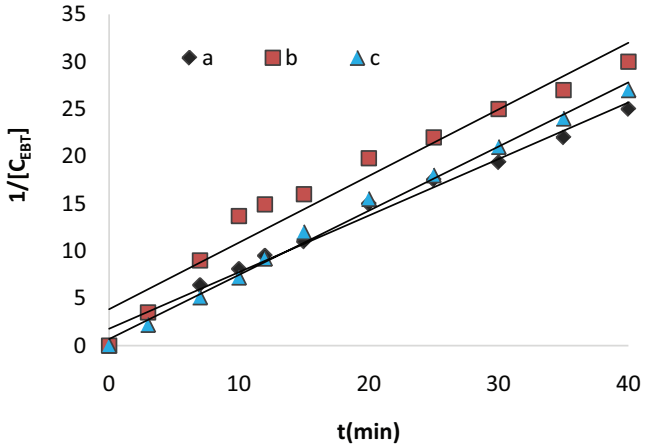

Fig. 11. Pseudo-second-order reaction kinetics for the degradation of EBT by a-Fe^{+2}/H_2O_2, b-Fe^{+2}/H_2O_2/Fe-MOF, c-Fe^{+2}/H_2O_2/Fe-ZIF (EBT 60 mg L^{-1}, Fe^{+2} = 16 mg L^{-1}, 0.004 g catalyst).

Table 2
Kinetic parameters for degradation of EBT by Fe^{+2}/H_2O_2, Fe^{+2}/H_2O_2/Fe-MOF and Fe^{+2}/H_2O_2/Fe-ZIF

Samples	First order		Second order	
	R^2	K_1 (min^{-1})	R^2	K_2 (g mg^{-1} min^{-1})
Fe^{+2}/H_2O_2	0.055	0.627	0.98	0.598
Fe^{+2}/H_2O_2/Fe-MOF	0.059	0.88	0.994	0.678
Fe^{+2}/H_2O_2/Fe-ZIF	0.065	0.645	0.947	0.703

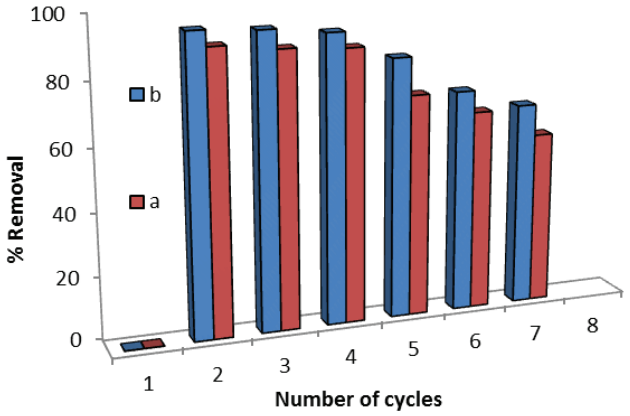

Fig. 12. Reusability and stability of catalyst (a-Fe-MOF, b-Fe-ZIF).

successive runs. However, the removal rate was rather comparable for all the runs at longer reaction times. It could be seen that the catalyst remain 86% EBT removal efficiency after four successive runs under the same reaction condition. The decrease of catalytic activity can be attributed to two reasons: first, the poisoning of the active catalytic sites due to the adsorbed organic species; second, the iron leaching may be another important factor that could cause the loss of activity of the catalyst

4. Conclusion

MOFs exhibit advantages on adsorption of dye molecules owing to high surface area and suitable pore size. One of the members in MOF, ZIF, has attracted much attention in recent days, and different kinds of ZIFs had been synthesized. In this research, Fe-MOF and Fe-ZIF were prepared and characterized. The results from FTIR, XRD and SEM methods confirmed the Fe-MOF and Fe-ZIF. They were successfully used as heterogen Fenton catalysts for the degradation of EBT. Various operating conditions were examined. The maximum degradation of EBT was occurred at 20 min of contact time, pH 3, 0.004 g catalyst and EBT of 60 mg L^{-1}. The experiments were verified at three different conditions (Fenton reaction, Fe^{+2}/H_2O_2), Fenton/MOF (Fe^{+2}/H_2O_2/Fe-MOF) and Fenton/ZIF (Fe^{+2}/H_2O_2/Fe-ZIF). The order of EBT removal was as followed: Fe^{+2}/H_2O_2, b-Fe^{+2}/H_2O_2/Fe-MOF, c-Fe^{+2}/H_2O_2/Fe-ZIF. The Fe-MOF and Fe-ZIF catalysts were reused.

Acknowledgments

We gratefully acknowledge financial support from the Research Council of Islamic Azad University of Yazd.

References

[1] C. Su, M. Pukdee-Asa, C. Ratanatamskul, M.C. Lu, Effect of operating parameters on decolorization and COD removal of three reactive dyes by Fenton's reagent using fluidized-bed reactor, Desalination, 278 (2011) 211–218.
[2] A. Berez, G. Schäfer, F. Ayari, M. Trabelsi-Ayadi, Adsorptive removal of azo dyes from aqueous solutions by natural bentonite under static and dynamic flow conditions, Int. J. Environ. Sci. Technol., 13 (2016) 1625–1640.
[3] R. Mahesh, M. Gadekar, A. Mansoor, Coagulation/flocculation process for dye removal using water treatment residuals: modelling through artificial neural networks, Desal. Wat. Treat., 57 (2016) 26392–26400.
[4] V. López-Grimau, M. Vilaseca, C. Gutiérrez-Bouzán, Comparison of different wastewater treatments for colour removal of reactive dye baths, Desal. Wat. Treat., 57 (2016) 2685–2692.
[5] N.M. Mahmoodi, Photodegradation of dyes using multiwalled carbon nanotube and ferrous ion, J. Environ. Eng., 139 1368–1374.
[6] B.M. Esteves, C.S.D. Rodrigues, R.A.R. Boaventura, F.J. Maldonado-Hodar, L.M. Madeira, Coupling of acrylic dyeing wastewater treatment by heterogeneous Fenton oxidation in a continuous stirred tank reactor with biological degradation in a sequential batch reactor, J. Environ. Manage., 166 (2016) 193–203.
[7] N. Inchaurrondoa, J. Fontb, C.P. Ramosc, P. Haure, Natural diatomites: efficient green catalyst for Fenton-like oxidation of Orange II, Appl. Catal., B, 181 (2016) 481–494.
[8] S. Hashemian, A. Foroghimoqhadam, Effect of copper doping on $CoTiO_3$Ilmenite type nano particles for removal of Congo red from aqueous solution, Chem. Eng. J., 235 (2014) 299–306.
[9] S. Hashemian, A. Dehghanpor, M. Moghahed, $Cu_{0.5}Mn_{0.5}Fe_2O_4$ nanospinels as potential sorbent for adsorption of brilliant green, J. Ind. Eng. Chem., 24 (2015) 308–314.
[10] S. Rodriguez, L. Vasquez, A. Romero, A. Santos, Dye oxidation in aqueous phase by using zero-valent iron as persulfate activator: kinetic model and effect of particle size, Ind. Eng. Chem. Res., 53 (2014) 12288–12294.
[11] S. Hashemian, M. Rahimi, A. Asghar Kerdegari, $CuFe_2O_4$@ graphene nanocomposite as a sorbent for removal of alizarine yellow azo dye from aqueous solutions, Desal. Wat. Treat., 57 (2016) 14696–14707.
[12] A. Alikarimi, S. Hashemian, M. Tabatabaee, Effect of calcination temperature of sawdust as a sorbent for bromo phenol red removal from aqueous solutions, Desal. Wat. Treat., 75 (2017)174–182.
[13] W.L. Ang, A.W. Mohammad, Y.H. Teow, A. Benamor, N. Hilal, Hybrid chitosan/$FeCl_3$ coagulation–membrane processes: performance evaluation and membrane fouling study in removing natural organic matter, Sep. Purif. Technol., 152 (2015) 23–31.
[14] N.P. Tantak, S. Chaudhari, Degradation of azo dyes by sequential Fenton's oxidation and aerobic biological treatment, J. Hazard. Mater., 136 (2006) 698–705.
[15] A. Maleki, H. Daraei, E. Amir Hosseini, S. Azizi, E. Faez, F. Gharibi, Azo dye DB71 degradation using ultrasonic-assisted Fenton process: modeling and process optimization, Arab. J. Sci. Eng., 40 (2015) 295–301.
[16] A.S Manjunatha, A. Sukhdev, Puttaswamy, Oxidative decolorisation of Eriochrome black T with Chloramine-T: kinetic, mechanistic, and spectrophotometric approaches, Color. Technol., 130 (2014) 340–348.
[17] A. Bedoui, M.F. Ahmadi, N. Bensalah, A. Gadri, Comparative study of Eriochrome black T treatment by BDD-anodic oxidation and Fenton process, Chem. Eng. J., 146 (2009) 98–104.

[18] F. Chen, W. Ma, J. He, J. Zhao, Fenton degradation of malachite green catalyzed by aromatic additives, J. Phys. Chem. A, 106 (2002) 9485–9490.
[19] H. Hassan, B.H. Hameed, Fenton-like oxidation of Acid Red 1 solutions using heterogeneous catalyst based on ball clay, Int. J. Environ. Sci. Develop., 2 (2011) 218–222.
[20] H. Hassan, B.H. Hameed, Oxidative decolorization of Acid Red 1 solutions by Fe–zeolite Y type catalyst, Desalination, 276 (2011) 45–52.
[21] H. Lim, J. Lee, S. Jin, J. Kim, J. Yoon, T. Hyeon, Highly active heterogeneous Fenton catalyst using iron oxide nanoparticles immobilized in alumina coated mesoporous silica, Chem. Commun., (2006) 463–465.
[22] W. Cheng, Y. Jiang, X. Li, Y. Li, X. Xu, K. Lin, Y. Wang, Fabrication and application of magnetic nanoreactor with multiple ultra-small cores and mesoporous shell in Fenton-like oxidation, Microporous Mesoporous Mater., 219 (2016) 10–18.
[23] M. Vallejo, P. Fernandez-Castro, M. Fresnedo. S. Roman, I. Ortiz, Assessment of PCDD/Fs formation in the Fenton oxidation of 2-chlorophenol: influence of the iron dose applied, Chemosphere, 137 (2015) 135–141.
[24] A. Dhakshinamoorthy, M. Alvaro, H. Garcia, Metal–organic frameworks as heterogeneous catalysts for oxidation reactions, Catal. Sci. Technol., 1 (2011) 856–867.
[25] A. Dhakshinamoorthy, A. M. Asiri, H. Garcia, Metal–organic frameworks as catalysts for oxidation reactions, Chem. A Europ. J., 2016, doi: 10.1002/chem.201505141.
[26] F. Farzaneh, L. Hamidipourm, Mn-metal organic framework as heterogenous catalyst for oxidation of alkanes and alkenes, J. Sci. I. R. Iran, 27 (2016) 31–37.
[27] J.P. Meng, Y. Gong, Q. Lin, M.M. Zhang, P. Zhang, H.F. Shi, J.H. Lin, Metal-organic frameworks based on rigid ligands as separator membranes in supercapacitor, Dalton Trans., 44 (2015) 5407–5416.
[28] Z. X. Li, G. Ye, J. Han, Y. Yang, K.Y. Zou, X. Wang, X.L. Wang, X.F. Gou, 1D-3D mixed-ligand frameworks with an unusual dmp topology tuned by intersection angles of isomeric benzenedicarboxylates: magnetic properties, gas-dependent calcination-thermolysis and energy storage performances, Dalton Trans., 44 (2015) 9209–9220.
[29] Y. Liu, P. Gao, C. Huang, Y. Li, Shape and size-dependent catalysis activities of iron-terephthalic acid metal-organic frameworks, Sci. China Chem., 58 (2015) 1553–1560.
[30] J. Liu, J. He, L. Wang, R. Li, P. Chen, X. Rao, L. Deng, L. Rong, J. Lei, NiO-PTA supported on ZIF-8 as a highly effective catalyst for hydrocracking of Jatropha oil, Sci. Rep., 6 (2016) 23667–23671.
[31] L.T.L. Nguyen, K.K.A. Le, N.T.S. Phan, A zeolite imidazolate framework ZIF-8 catalyst for Friedel-Crafts acylation, Chin. J. Cat., 33 (2012) 688–696.
[32] K.Y. Lin, H.A. Chang, Zeoliticimidazoleframework-67(ZIF 67) as a heterogeneous catalyst to activate peroxy mono sulfate for degradation of rhodamine B in water, J. Taiwan Inst. Chem. Eng., 53 (2015) 40–45.
[33] S. Dadfarnia, A.M. Haji Shabani, S.E. Moradi, S. Emami, Methyl red removal from water by iron based metal-organic frameworks loaded onto iron oxide nanoparticle adsorbents, Appl. Surf. Sci., 330 (2015) 85–93.
[34] E. Dixon dikio, A.M. Farah, Synthesis, characterization and comparative study of copper and zinc metal organic frameworks, Chem. Sci. Trans., 2 (2013) 1386–1394.
[35] G. Song, Z. Wang, L. Wang, G. Li, M. Huang, F. Yin, Preparation of MOF (Fe) and its catalytic activity for oxygen reduction reaction in an alkaline electrolyte, Chin. J. Catal., 35 (2014) 185–195.
[36] M. Zahmakıran, S. Özkar, M. Yurderi, M. Gülcan, Ruthenium(0) nanoparticles stabilized by metal-organic framework (ZIF-8): highly efficient catalyst for the dehydrogenation of dimethylamine-borane and transfer hydrogenation of unsaturated hydrocarbons using dimethylamine-borane as hydrogen source, Appl. Catal., B, 160–161 (2014) 534–551.
[37] S. Hashemian, B. Sadeghi, M. Mangeli, Hydrothermal synthesis of nano cavities of Al-MCF for adsorption of indigo carmine from aqueous solution, J. Ind. Eng. Chem., 21 (2015) 423–427.
[38] J.P. Thielemann, F. Girgsdies, R. Schlögl, C. Hess, Pore structure and surface area of silica SBA-15: influence of washing and scale-up, Beilstein J. Nanotechnol., 2 (2011) 110–118.
[39] F. Azimov, I. Markova, V. Stefanova, Kh. Sharipov, Synthesis and characterization of SBA-15 AND Ti-SBA-15 nanoporous materials for DME catalysts, J. Univ. Chem. Technol. Metall., 47 (2012) 333–340.
[40] H. Zhang, H. Fu, D. Zhang, Degradation of C.I. Acid Orange 7 by ultrasound enhanced heterogeneous Fenton-like process, J. Hazard. Mater., 172 (2009) 654–660.
[41] X. Sun, T. Kurokawa, M. Suzuki, M. Takagi, Y. Kawase, Removal of cationic dye methylene blue by zero-valent iron: effects of pH and dissolved oxygen on removal mechanisms, J. Environ. Sci. Health A Tox. Hazard. Subst. Environ. Eng., 50 (2015) 1057–1071.
[42] M. Ahmad, A. Asghar, A.A. Abdul Raman, W.M.A. Wan Daud, Enhancement of treatment efficiency of recalcitrant wastewater containing textile dyes using a newly developed iron zeolite socony Mobil-5 heterogeneous catalyst, PLOS one, (2015) 1–23. doi: 10.1371/journal.pone.0141348.
[43] M.B. Kasiri, H. Aleboyah, A. Aleboyah, Degradation of Acid Blue 74 using Fe-ZSM5 zeolite as a heterogeneous photo-Fenton catalyst, Appl. Catal., B, 84 (2008) 9–15.